

A Figure-of-Merit for Design of High Performance Inductive Power Transmission Links for Implantable Microelectronic Devices

Mehdi Kiani, *IEEE Student Member*, and Maysam Ghovanloo, *IEEE Senior Member*

Abstract— Wireless power transfer through inductive coupling is used in many applications such as high performance implantable microelectronic devices (IMDs). Power transfer efficiency (PTE) and power delivered to the load (PDL) are two conventional inductive link design merits that determine the energy source and driver specifications, heat dissipation, power transmission range, and risk of interference with other devices. Unfortunately designing the inductive link to achieve a high PTE will drastically reduce the PDL and vice versa. Therefore, we are proposing a new figure-of-merit (FoM), which includes both PTE and PDL with proper weights, to help designers of inductive power transfer links to strike a balance between high PTE and PDL at the same time. Three design examples based on the PTE, PDL, and the new FoM have been presented for IMDs to demonstrate the usage and efficacy of the FoM. Our measurement results show that the inductive link optimized based on the FoM can achieved 1.65 times higher PTE than the one optimized for the PDL (72.5% vs. 44%) and at the same time provide 20.8 times larger PDL compared to the one optimized for the PTE (177 mW vs. 8.5 mW for 1 V driving voltage). The inductive links optimized for the PTE and PDL provide 24% higher PTE and PDL compared to the one optimized based on the FoM, respectively.

I. INTRODUCTION

INDUCTIVE power transmission received considerable attention as the most feasible way to power up low, medium, and high frequency radio frequency identification (RFID) transponders and some implantable microelectronic devices (IMD), such as cochlear implants due to size, weight, and lifetime limitations in batteries [1], [2]. In these systems, a highly efficient power amplifier (PA) on the transmitter side (Tx) drives the primary coil, which is mutually coupled to a secondary coil on the receiver side (Rx) and drives the load, R_L , as shown in Fig. 1a.

A key design requirement in inductive links for IMD applications is to have sufficient power delivered to the load (PDL) while maintaining high power transfer efficiency (PTE). When R_L is constant, the PDL would be equivalent to the inductive link voltage gain all the way from the source to the load. High PTE is required to reduce 1) the heat dissipation within the coils, 2) tissue exposure to the AC magnetic field, which can cause additional heat dissipation, 3) size of the main energy source, and 4) interference with nearby electronics to satisfy regulatory requirements [3], [4]. At the same time, the link should deliver sufficient power to

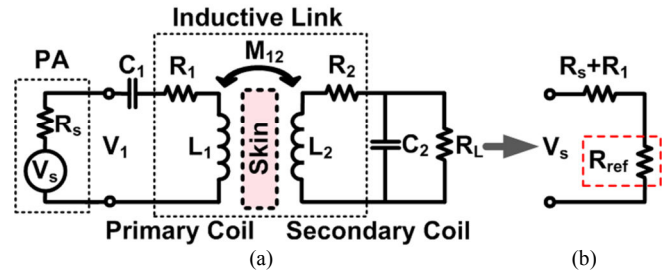


Fig. 1. (a) Lumped circuit model of the inductive power transmission link with the PA loss modeled with R_s , (b) Equivalent circuit at resonance showing the reflected load from secondary onto the primary loop.

the load while considering practical limitations of the energy source and the PA. Increasing the source voltage, V_s in Fig. 1a, to increase the PDL can reduce the driver efficiency, require larger transistors in the PA, and raise safety issues.

Several methods have been proposed before for designing efficient power transmission links. In [5]-[7], geometries of the primary and secondary coils, L_1 and L_2 in Fig. 1a, have been optimized to achieve the maximum voltage on the load (\sim PDL). PDL is a key design merit because powering the IMDs is a major challenge when coils are miniaturized. On the other hand, design and geometrical optimization of the inductive power transmission links based on the PTE have been widely studied [8]-[11]. A different approach has been adopted in [12], in which L_2 is first designed to achieve the maximum PTE for a given R_L , and then L_1 geometry is optimized to achieve the desired voltage gain from source to load, and consequently the PDL. It is, therefore, clear that the literature still lacks a figure-of-merit (FoM) that incorporates both PTE and PDL, based on which practical power transmission links can be designed and optimized.

In this paper, we propose a new FoM, which guides designers towards inductive power transfer links with the highest possible PTE and PDL. In the following section we have introduced the new FoM and the trade-offs between achieving high PTE and PDL, simultaneously. Section III presents the calculation and measurement results of three sets of inductive links designed based on the PTE, PDL, and the new FoM for IMD applications followed by the concluding remarks in section IV.

II. A NEW FOM FOR INDUCTIVE POWER TRANSMISSION

Fig. 1a shows the simplified schematic diagram of an inductive power transmission link, including the power amplifier (PA), which is modeled with the driving voltage source, V_s , and the PA loss, R_s . Key parameters that affect the design of this link from the energy source to the load are: R_s , V_s , power required by the load (P_L), PA supply voltage

This work was supported in part by the National Institutes of Health (NIBIB) grants 1R01NS062031-01A1 and 1R21EB009437-01A1, as well as the National Science Foundation under award ECCS-824199. Mehdi Kiani and Maysam Ghovanloo* are with the GT-Bionics Lab, School of Electrical and Computer Engineering at Georgia Institute of Technology, Atlanta, GA, USA (e-mail: mgh@gatech.edu).

(V_{DD}), PA transistor breakdown voltage, and safety limits for the application [9].

In a class-E PA, zero-voltage-switching allows for high power efficiency with peak voltages across the primary coil and the PA transistor that are 1.07 and 3.56 times V_{DD} , respectively [13]. Therefore, when the application involves a large P_L , R_s should be reduced to provide sufficient available power from the source, $P_{av} = V_s^2/8R_s$, at reasonable V_s and V_{DD} . However, utilizing large transistors to reduce R_s results in increased dynamic switching losses in the PA [12]. Therefore, the power transmission link should be designed such that it achieves high PTE and also provides sufficient PDL considering all practical limitations on the driver.

It can be shown that the highest PTE and PDL for the inductive link, shown in Fig. 1a, can be achieved when both LC tanks are tuned at the same resonance frequency, $f_0 = 1/2\pi\sqrt{L_1C_1} = 1/2\pi\sqrt{L_2C_2}$ [12]. The effect of the secondary side on the primary side can be modeled at resonance with the reflected impedance,

$$R_{ref} = k_{12}^2 \omega_0 L_1 Q_{2L}, \quad (1)$$

where $k_{12} = M_{12}/\sqrt{L_1 L_2}$, M_{12} is the mutual inductance between L_1 and L_2 , and $Q_{2L} = Q_2 Q_L / (Q_2 + Q_L)$, in which $Q_2 = \omega_0 L_2 / R_2$ and $Q_L = R_L / \omega_0 L_2$, which is often referred to as the load quality factor [1]. At resonance, the primary loop can be simplified to the circuit shown in Fig. 1b.

To derive an equation for the PTE, η , at resonance, we should consider that the power provided by the PA (V_s) divides between $R_s + R_1$ and R_{ref} , and the power delivered to R_{ref} , i.e. the power that is received by the secondary loop, divides between R_2 and R_L , which are the only power consuming components on the Rx side. These assumptions lead to

$$\eta = \frac{R_{ref}}{R_s + R_1 + R_{ref}} \cdot \frac{Q_{2L}}{Q_L} = \frac{k_{12}^2 Q_1 Q_{2L}}{1 + k_{12}^2 Q_1 Q_{2L}} \cdot \frac{Q_{2L}}{Q_L}, \quad (2)$$

where $Q_1 = \omega_0 L_1 / (R_s + R_1)$ [12]. The first and second terms in (2) correspond to the power division between $R_s + R_1$ and R_{ref} , and R_2 and R_L , respectively. Therefore, it can be seen from (2) that to achieve the highest PTE, R_{ref} should be maximized.

PDL can be calculated by multiplying the power provided by V_s , i.e. $V_s^2/2(R_s + R_1 + R_{ref})$, with the PTE from (2)

$$P_L = \frac{V_s^2 R_{ref}}{2(R_s + R_1 + R_{ref})} \cdot \frac{Q_{2L}}{Q_L} = \frac{V_s^2}{2(R_s + R_1)} \frac{k_{12}^2 Q_1 Q_{2L}}{(1 + k_{12}^2 Q_1 Q_{2L})^2} \cdot \frac{Q_{2L}}{Q_L} \quad (3)$$

It can be seen from (3) that PDL does not necessarily increase by maximizing R_{ref} . Taking the derivative of (3) with respect to R_{ref} , the maximum PDL at a certain coupling distance, d_{12} , is achieved when $R_{ref} = R_s + R_1$. Under this impedance-matched condition, the PTE is always less than 50%, because half of the power is dissipated in $R_s + R_1$.

In this paper, we propose a new figure-of-merit (FoM) for

the design of inductive power transmission links:

$$FoM = \frac{\eta^n \times P_L}{V_s^2} = \frac{\eta^{n+1}}{2(R_s + R_1 + R_{ref})} \quad (4)$$

where n depends on the PDL that is required in a particular application, to be discussed in the following. Interestingly, this FoM is in Siemens, which implies how conductive the inductive link is to electric power. The inductive link FoM can be linked to other circuit parameters in Fig. 1 by substituting (2) and (3) in (4)

$$FoM = \frac{(k_{12}^2 Q_1 Q_{2L})^{n+1}}{2(R_s + R_1)(1 + k_{12}^2 Q_1 Q_{2L})^{n+2}} \cdot \left(\frac{Q_{2L}}{Q_L}\right)^{n+1} \quad (5)$$

The PTE profile of the inductive link according to (2) is a monotonically decreasing function of the coils' coupling distance, d_{12} . However, the PDL and FoM profiles are maximized at a particular d_{12} that can be found by calculating the derivatives of (3) and (5), respectively, with respect to k_{12}

$$k_{12,PDL} = \left(\frac{1}{Q_1 Q_{2L}}\right)^{1/2}, \quad k_{12,FoM} = \left(\frac{n+1}{Q_1 Q_{2L}}\right)^{1/2} \quad (6)$$

By substituting $k_{12,FoM}$ in (2) and (3), one can find the PTE and PDL of the inductive link when the FoM is maximized at that particular d_{12} without any further constraints on the coils' geometries. This will lead to

$$\eta_{FoM} = \frac{n+1}{n+2} \cdot \frac{Q_{2L}}{Q_L}, \quad P_{L,FoM} = \frac{V_s^2}{2(R_s + R_1)} \cdot \frac{n+1}{(n+2)^2} \cdot \frac{Q_{2L}}{Q_L} \quad (7)$$

The proposed FoM in (4) reduces to PTE if $n \rightarrow \infty$, and to PDL if $n = 0$. Therefore, the maximum achievable PTE and PDL at a particular d_{12} can be calculated from (7) by substituting n with ∞ and 0, respectively.

$$\eta_{max} = \frac{Q_{2L}}{Q_L}, \quad P_{L,max} = \frac{V_s^2}{8(R_s + R_1)} \cdot \frac{Q_{2L}}{Q_L} \quad (8)$$

Using (7) and (8), we can calculate the percentage of the PTE and PDL that the inductive link should forfeit when it is designed based on the optimal FoM,

$$\eta_{Loss} = \frac{\eta_{max} - \eta_{FoM}}{\eta_{max}} = \frac{1}{n+2}, \quad P_{L,Loss} = \frac{P_{L,max} - P_{L,FoM}}{P_{L,max}} = \frac{n^2}{(n+2)^2} \quad (9)$$

Fig. 2 shows the PTE and PDL losses vs. n , based on (9). The key points to be learned from these curves are: 1) If the inductive link is optimized for the PDL, i.e. $n = 0$, it loses 50% of the PTE. 2) If the inductive link is optimized for the PTE, i.e. $n \rightarrow \infty$, it loses 100% of the PDL. However in practice, the application and coil fabrication constraints limit the PTE and allow a small amount of power to be delivered to the load ($PDL > 0$). 3) When $n = 2$, the amounts of both PTE and PDL losses are equal to 25%.

In a particular application, it is often possible to determine whether the PTE, PDL, or both are important. The designer

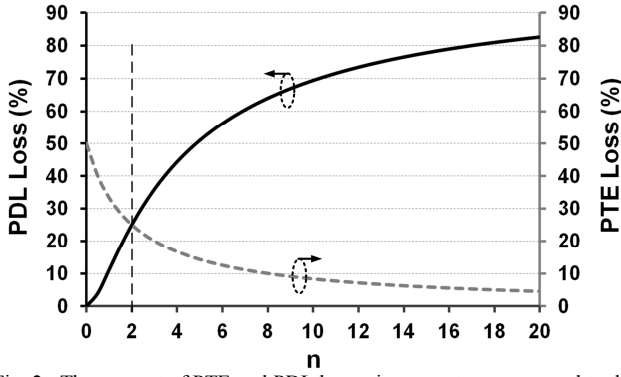


Fig. 2. The amount of PTE and PDL losses in percentage compared to the maximum possible value vs. n when the inductive link is designed to maximize the proposed FoM in (4) as opposed to the PTE or PDL. It can be seen that $n = 2$ results in similar PTE and PDL losses equals to 25%.

can choose a suitable n , according to Fig. 2, and design the inductive link by maximizing the proposed FoM in (4).

We believe $n = 2$ works best for most applications that need large PDL, considering practical driver limitations discussed earlier. Even though in the rest of this paper we consider $n = 2$, our discussions are applicable to any desired n in the FoM (4).

III. COMPARISON BETWEEN INDUCTIVE LINKS DESIGNED BASED ON FOM, PTE, AND PDL

In this section, we have compared the performance of three different sets of inductive links, designed based on the PTE, PDL, and the new FoM for IMD applications. Measurement results have also been provided to verify the accuracy of our theoretical models and calculations.

A. Inductive Link Design Procedure

All design examples are based on wire-wound coils (WWC) made of single filament solid wires. We have used the same design procedure, described in [11] for optimization of the PTE in printed spiral coils (PSC) with the following modifications: 1) The PSC fill factors (Φ_1 and Φ_2) were replaced with the WWC number of turns (n_1 and n_2). 2) (2), (3), and (5) were used in the design flow to maximize the PTE, PDL, and FoM, respectively. 3) The relationship between the inductive link parameters, such as k and Q , and the WWC geometries were obtained from [14].

For the IMD design example, we considered a retinal implant with the following assumptions: L_1 and L_2 were considered circular-shaped WWCs, operating at 13.56 MHz. The link was designed to deliver 250 mW to an $R_L = 100 \Omega$ from a nominal coupling distance of $d_{12} = 10$ mm via a driver (PA) with output resistance of $R_s = 0.5 \Omega$. L_2 outer diameter and the maximum wire diameter were $D_{o2} = 10$ mm and $w_{2,max} = 0.64$ mm (AWG22), respectively, to limit the implant size, thickness, and weight. Moreover, L_1 maximum wire diameter was limited to $w_{1,max} = 1.6$ mm (AWG14) to limit its weight with respect to the electronics [9].

B. Calculation vs. Measurement Results

Table I summarizes the results of the design procedure in [11] for three sets of inductive links optimized based on the

TABLE I
THE INDUCTIVE LINK SPECIFICATIONS FOR PTE, PDL AND FOM OPTIMIZATION

Parameters		Symbols	Optimized Parameter		
			PTE	PDL	FoM
L_1	Inductance (μH)	L_1	2.4	0.072	0.13
	Outer diameter (mm)	D_{o1}	41	13	21.5
	Wire diameter (mm)	w_1	1.6		
	Num. of turns	n_1	10	3	2
	Line spacing (μm)	s_1	100		
	Quality factor	Q_1	171.8	12.1	21.2
L_2	Inductance (μH)	L_2	0.022		
	Outer diameter (mm)	D_{o2}	10		
	Wire diameter (mm)	w_2	0.64		
	Num. of turns	n_2	1		
	Line spacing (μm)	s_2	100		
	Quality factor	Q_2	1486		
$L_1 - L_2$ coupling distance (mm)		d_{12}	10		
Max. wire diam. of L_1 / L_2 (mm)		$w_{1,2,max}$	1.6 / 0.64		
Nominal source resistance (Ω)		R_s	0.5		
Nominal load (Ω)		R_L	100		
Power carrier frequency (MHz)		f_0	13.56		
Power transfer efficiency (%)		η	90.2	44	72.5
Power delivered to load (mW)		P_L	8.5	220	177
Figure-of-Merit ($\text{m}\Omega^{-1}$)		FoM	6.9	42.6	93

Q_2 also includes $R_s = 0.5 \Omega$.

Grayed rows indicate the design constraints.

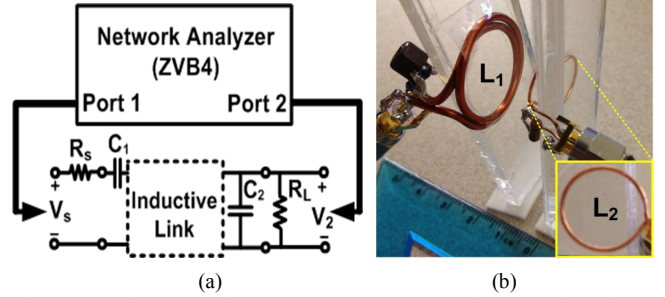


Fig. 3. (a) The PTE and PDL measurement setup using network analyzer with all the coils tuned at the carrier frequency, and both R_s and R_L connected in the setup, (b) The inductive link optimized based on the FoM and used to measure the PTE and PDL. Coil specs are listed in Table I.

PTE, PDL, and FoM. Fig. 3a shows the measurement setup proposed in [14] to measure the PTE and PDL of an inductive link accurately. The FoMs are then calculated from (4) for $n = 2$. The network analyzer is used to measure the S-parameters and consequently the Z-parameters of the inductive link with both R_s and R_L connected in the setup. The PTE and PDL are then found from the 2-port equations

$$PTE = \frac{|Z_{21}|^2}{R_L |Z_{11}| \cos(\angle Z_{11})}, \quad PDL = \frac{|V_s|^2}{2R_L |Z_{11}|^2} |Z_{21}|^2. \quad (10)$$

Fig. 3b shows the experimental setup for measuring the PTE and PDL of the inductive link that was optimized for the FoM. These coils were fabricated based on the values listed in Table I, and held in parallel and perfectly aligned using non-conducting Plexiglas supports.

Figs. 4a and 4b show the differences between calculated and measured results for the PTE, PDL, and FoM of the three sets of WWCs specified in Table I. It can be seen in Fig. 4a that the link optimized based on the FoM has not only achieved 1.65 times more PTE than the one optimized based on the PDL (72.5% vs. 44%) but also provided 20.8

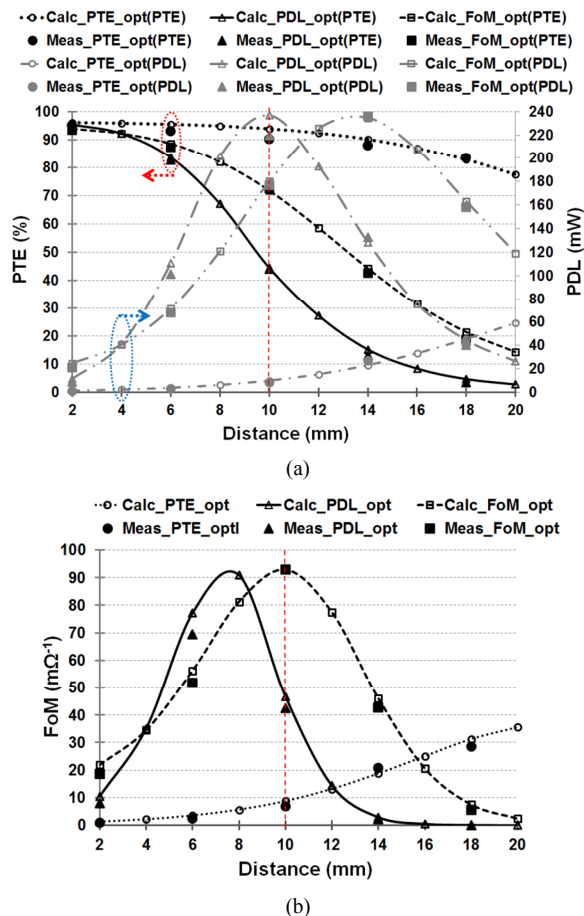


Fig. 4. Comparison between three sets of 2-coil links optimized for PTE, PDL, and FoM vs. coupling distance, d_{12} . $R_s = 0.5 \Omega$ and $R_L = 100 \Omega$. a) The calculated and measured values of the PTE and PDL for $V_s = 1 \text{ V}$ b) The FoM values defined in (4) for $n = 2$. The inductive links' specifications for the nominal distance of $d_{12} = 10 \text{ mm}$ are summarized in Table I.

times larger PDL compared to the one optimized based on the PTE (177 mW vs. 8.5 mW for $V_s = 1 \text{ V}$). This leads to driving voltages of $V_s = 5.4 \text{ V}$, 1.06 V, and 1.19 V and peak voltages across the PA transistor of 19.2 V, 3.8 V, and 4.2 V for the PTE-, PDL-, and FoM-optimized links, respectively, when delivering 250 mW to the load with a class-E PA [13].

These results clearly show the stringent requirements on the driver of the links with low FoM. For instance, on-chip PA transistors in most advanced IC fabrication processes, which have low breakdown voltages, cannot be used in the PTE-optimized link to reduce the Tx size and increase the driver efficiency. It should be noted that the FoM-optimized link achieves a high performance at the cost of only 24% drop in the PTE and PDL compared to the PTE- and PDL-optimized links. This was slightly less than the theoretical 25% due to measurement errors and our WWC fabrication constrains. Therefore, unless the application requires only a small PDL, the inductive link that is designed based on the proposed FoM is superior by simultaneously providing high PTE and PDL. Moreover, comparing the FoMs of the three sets of links in Fig. 4b shows that the link that is optimized based on the proposed FoM maintains the highest performance for a wide range of coupling variations.

It should be noted that the slight discrepancies between the calculated and measured PTE and PDL values are due to the limited Q of the capacitors and measurement setup non-idealities. The FoM calculated from the measured PTE and PDL show slightly more error because the PTE and PDL errors accumulate in the $FoM = \eta^2 \times P_L$ ($V_s = 1 \text{ V}$).

IV. CONCLUSION

A new figure-of-merit (FoM) has been proposed to design high performance inductive power transmission links. We have demonstrated the tradeoffs between maximizing the PTE, PDL, and both of them together to help designers choose the optimal design merits for a particular application. Three sets of inductive links for an IMD application were designed based on the PTE, PDL, and FoM to show the efficacy of the proposed FoM. Measurement results showed that the link optimized for the FoM not only achieves PDL levels close to that of the link optimized for the PDL but also provides significantly higher PTE. This will relax the driver design by reducing the supply and peak voltage levels on the PA transistor. Our future work will focus on using the proposed FoM to differentiate between 2-, 3-, and 4-coil inductive links for a given application [14].

REFERENCES

- [1] K. Finkenzerler, *RFID-Handbook*, 2nd ed. Hoboken, NJ: Wiley, 2003.
- [2] G. M. Clark, *Cochlear Implants: Fundamentals and Applications*. New York: Springer-Verlag, 2003.
- [3] G. Lazzi, "Thermal effects bioimplants," *IEEE Eng. Med. Biol. Mag.*, vol. 24, pp. 75-81, Sep. 2005.
- [4] *IEEE Standard for Safety Levels With Respect to Human Exposure to Radio Frequency Electromagnetic Fields, 3 kHz to 300 GHz*, IEEE Standard C95.1, 1999.
- [5] W. J. Heetderks, "RF powering of millimeter and submillimeter-sized neural prosthetic implants," *IEEE Trans. Biomed. Eng.*, vol. 35, no. 5, pp. 323-327, May 1988.
- [6] C. R. Neagu, H. V. Jansen, A. Smith, J. G. E. Gardeniers, and M. C. Elwanspoek, "Characterization of a planar microcoil for implantable microsystems," *Sens. Actuat. A*, vol. 62, pp. 599-611, July 1997.
- [7] S.C.Q. Chen and V. Thomas, "Optimization of inductive RFID technology," in *Proc. IEEE Int. Symp. Electron. Environ.*, pp. 82-87, May 2001.
- [8] C. Zierhofer and E. Hochmair, "High-efficiency coupling-in sensitive transcutaneous power and data transmission via an inductive link," *IEEE Trans. Biomed. Eng.*, vol. 37, no. 7, pp. 716-722, Jul. 1990.
- [9] G. A. Kendir, W. Liu, G. Wang, M. Sivaprakasam, R. Bashirullah, M. S. Humayun, and J. D. Weiland, "An optimal design methodology for inductive power link with class-E amplifier," *IEEE Trans. on Circuits and Systems I*, vol. 52, pp. 857-866, May 2005.
- [10] R. R. Harrison, "Designing efficient inductive power links for implantable devices," *IEEE International Symposium on Circuits and Systems*, pp. 2080-2083, May 2007.
- [11] U. M. Jow, and M. Ghovanloo, "Design and optimization of printed spiral coils for efficient transcutaneous inductive power transmission," *IEEE Trans. Biomed. Cir. Syst.*, vol. 1, pp. 193-202, Sep. 2007.
- [12] M. W. Baker and R. Sarpeshkar, "Feedback analysis and design of RF power links for low-power bionic systems," *IEEE Trans. Biomed. Cir. Syst.*, vol. 1, no. 1, pp. 28-38, Mar. 2007.
- [13] M. K. Kazimierczuk, and D. Czarkowski, *Resonant Power Converters*, NY: Wiley-Interscience, 1995.
- [14] M. Kiani, U. Jow, and M. Ghovanloo, "Design and optimization of a 3-coil inductive link for efficient wireless power transmission," *IEEE Trans. Biomed. Cir. Syst.*, vol. 5, pp. 579-591, Dec. 2011.